Does the Incoming Oxygen Atom Influence the Geometries and the Electronic and Magnetic Structures of Co_n Clusters?

Li Liu, Run-Ning Zhao, Ju-Guang Han,* Fu-Yi Liu, Guo-Qiang Pan, and Liu-Si Sheng

National Synchrotron Radiation Laboratory, University of Science and Technology of China, Hefei 230029, People's Republic of China

Received: September 10, 2008; Revised Manuscript Received: November 14, 2008

The small-sized Co_nO ($n = 1-5$) clusters with different spin states have been systematically investigated by using the density-functional approach. The total energies, equilibrium geometries, and magnetic properties are discussed. Equilibrium geometries and the relative stabilities in terms of the calculated fragmentation energies are discussed, manifesting that the remarkable stable small-sized cluster corresponds to the Co_2O isomer, and that the O atom prefers the surface-capped pattern on Co_n ($n > 2$) clusters and bonds with three Co atoms simultaneously. Furthermore, the calculated averaged atomic magnetic moments of Co_nO ($n = 1-5$) clusters exhibit that the septet Co_2O structure has the biggest averaged atomic magnetic moment of 2.0 μ_B/atom, it is interesting that the oxygen capped Co_n ($n = 1-5$) clusters retain the magnetic properties of bare transition metal (TM) Co_n clusters. In addition, the distribution of electron density of the HOMO states for the most stable Co_nO clusters mainly localizes around Co_n atoms while the distribution around O atom is very low, and their shapes of the HOMO and bonding properties between bare Co_n clusters and Co_nO clusters are obviously different. The calculated electron affinities and experimental results (*J. Phys. Chem. A* **2002**, *106,* 4891) show that the incoming oxygen atom causes a minor influence on the electronic properties of Co_n clusters. Comparisons of the calculated ionization potentials (IPs) for CoO and Co_2O clusters with available experimental measurements are made.

1. Introduction

In recent years, transition metal (TM) oxide clusters have gained increasing interest both in theoretical and experimental fields, and have become a new research field because they play a prominent role in environmental processes, catalytic activity, and materials sciences; and they exhibit noval electronic, magnetic, optical, and chemical properties.[1−13] Although there are many studies of the mass spectrometry and their photoelectronspectroscopy of TM oxides, determining the relative stabilities of these systems remains problematic. TM oxide cluster experiments in the gas phase have contributed fundamental information needed to reveal properties such as chemical bonding, reactivity, and magnetic and electronic properties. Theoretical investigations have combined with such experimental results to probe the geometries and stabilities of small TM oxide clusters.

In the past decades, theoretical and experimental investigations on cobalt oxides mainly focused on neutral and ionic cobalt monoxides.[14−31] The size-dependent chemistry and kinetics of gas-phase reactions of the small-sized Co_n^+ ($n = 2-9$) with O_2 are examined by using a selected ion drift tube with laser vaporization source;[25] and the kinetic-energy dependence for the reactions of different sized Co_n^+ ($n = 2-20$) with O_2 is measured as a function of kinetic energy over a range of 0 to 10 eV in a guided ion-beam tandem mass spectrometer. The reaction kinetics of small Co_n ($n = 2-8$) clusters toward O_2 using a flow tube experiment are studied, showing that the reactive rate coefficients are largely independent of the cluster size.[28] Moreover, a variety of Co_n^+, Co_nO^+, and $Co_nO_2^+$ (Co_nO_m clusters, $m \leq n$) product ions is observed experimentally.[11] In addition, the oxide chemistry of both dimeric and trimeric transition-metal cluster ions containing iron and cobalt atoms in the gas phase by using Fourier transform mass spectrometry (FTMS) is discussed.[26] Furthermore, a combined IR matrix isolation and theoretical studies of the formation and structure of CoO_2 have been reported,[27] and the basic electronic and geometrical properties of cobalt dioxide are explored theoretically. In addition, the mass selected cobalt oxide cluster anions $Co_nO_m^-$ ($n = 4-20$, $m = 0-2$) by using photodetachment photoelectron spectroscopy (PES) are studied, and the size-dependent evolution of the electronic structure of the cobalt oxide clusters is discussed in terms of the composition of clusters. Threshold binding energy features are mainly contributed from Co d-derived orbitals throughout the complete series, indicating that the incoming O atom causes a minor influence on the electronic structures.[29] The ground and low-lying excited states of CoO_4, together with electronic structures of the 3d metal monoxide anions, are studied theoretically.[30,31]

The Co_nO clusters have complicated electronic and magnetic properties due to the 3d subshells, and their energetic difference between different spin states is close, therefore, the determination of the ground state is a complicated and challenging work. To our knowledge, however, there are no systematic theoretical investigations on small-sized oxygen doped cobalt clusters. Stimulated by the experimental observations of ref 11 above, we provide a detailed theoretical investigation of the equilibrium geometries, relative stabilities, fragmentation energies [$D(n,n-1)$], the averaged atomic binding energies [$E_b(n)$], and magnetic properties of small-sized Co_nO clusters; comparison with available experimental and theoretical results is made.

---

* To whom correspondence should be addressed. E-mail: jghan@ustc.edu.cn. Fax: +86-551-5141078.

10.1021/jp8080244 CCC: $40.75

2. Computational Details

The geometry optimizations of Co_nO ($n = 1-5$) clusters are performed by using density-functional theory (DFT) with the unrestricted B3LYP exchange-correlation potential,[32,33] and the GEN basis sets, which are the combinations of LanL2DZ and 6-31G(d,p) basis sets,[34] are employed for the respective Co and O atoms. The standard LanL2DZ basis sets are employed to provide an effective way to reduce difficulties in calculations of two-electron integrals caused by transition metal Co atom.[8,35]

As the number of isomers is increased quickly with the size of clusters, there are abundant low-lying isomers with energies near the ground state, and it is difficult to find the ground state of clusters simply according to the calculated total energies of the isomers.[8] In order to obtain the lowest-energy Co_nO structures, we have chosen a considerable number of possible structures as initial geometries for each cluster size ($n = 1-5$). Based upon the previous available theoretical or experimental Co_n geometries, different evolution patterns for determining the Co_nO isomers, including O-substituted, O-concaved patterns, and Co-capped patterns, are first taken into account,[36-38] and then the equilibrium geometry is determined by varying the geometry starting from high-symmetry geometry to low-symmetry geometry. This leads to a limited number of possible stable structures for each size of clusters. For each stationary point of a cluster, the stability is reassured by the calculated harmonic vibrational frequencies. If the unstable geometry with one imaginary vibrational frequency is yielded, a relaxation along the coordinates of the imaginary vibrational mode is rearranged until a true local minimum is actually obtained.[8] Consequently, the geometries and total energies for each stable cluster and its stable isomers in this article correspond to the local minima. In addition, geometries with the most stable quartet Co atom, septet Co_2, octet Co_3, nonet Co_4, and Co_5 with spin $S = 11/2$ are calculated and listed in Figure 1.

The doublet, quartet, and sextet spin states for n-odd members are considered while the singlet, triplet, and quintuplet spin states correspond to n-even members of series. In cases when the total energy decreases with increasing spin S, we consider increasingly higher spin states until the energy minimum with respect to S is reached. The spin contamination for oxygen doped cobalt clusters with high spin states is nonnegligible, and it is found to be about 8% and thus relatively high in some uints.

In order to test the reliability of our calculation, the calculated bond length, electron affinity, and the lowest harmonic vibrational frequencies of Co_2 and CoO dimers are listed in Table 1. Based upon the calculated values of Co_2, and CoO dimers, a good agreement with the experimental and theoretical results that are available is reached,[39-45] indicating that our calculations are reliable and accurate and the UB3LYP/GEN method will actually provide reliable data of Co_nO ($n = 1-5$) clusters. All theoretical calculations are carried out with the Gaussian 03 program package.[46]

3. Results and Discussions

3.1. Geometries and Stabilities. ***CoO.*** The $C_{\infty v}$ CoO geometry with different spin states is optimized at the UB3LYP/GEN level. The total energies of the CoO cluster with spin $S = 1/2$, 3/2, and 5/2 are respectively -220.1392829, -220.1970188, and -220.17457 hartrees; The corresponding Co−O bond length of CoO cluster is of 1.606, 1.595, and 1.688 Å, respectively. This feature is shown to be associated with the stability of the CoO cluster as spin S varies from $S = 1/2$ to 5/2. Obviously, the doublet and sextet states are higher by respectively 1.571 and 0.611 eV in total energies than the quartet state. Therefore, the quartet CoO cluster is the most stable structure, which is selected as the ground state with electronic state of $^4\Delta$. Additionally, the calculated Co−O bond length, electron affinity, and adiabatic ionization potential for CoO dimer at the B3LYP level are in good agreement with the experimental results (Table 1).[11,43,44] Especially, the calculated harmonic frequency is 942.9 cm^{-1}; comparison with the previous high-level theoretical calculation on the CoO dimer (909 cm^{-1}) is made.[24] Finally, the calculated natural popualtions exhibit that the ionized charge in CoO^+ dimer is mainly from the cobalt atom, reflecting that our findings are in good agreement with previous experimental prediction.[11] Thus, the comparisons of our calculated results with the experimental results give additional support to the use of the B3LYP method in the present context as shown below.

Co_2O. All the possible geometries are considered based upon the most stable septet Co_2 dimer, four stable isomers, which are shown in Figure 1, have been identified for the ground-state candidates of Co_2O clusters. Based upon the calculated total energy listed in Table 2, the closed isosceles triangular septet C_{2v} Co_2O 2a geometry is the lowest-energy structure with

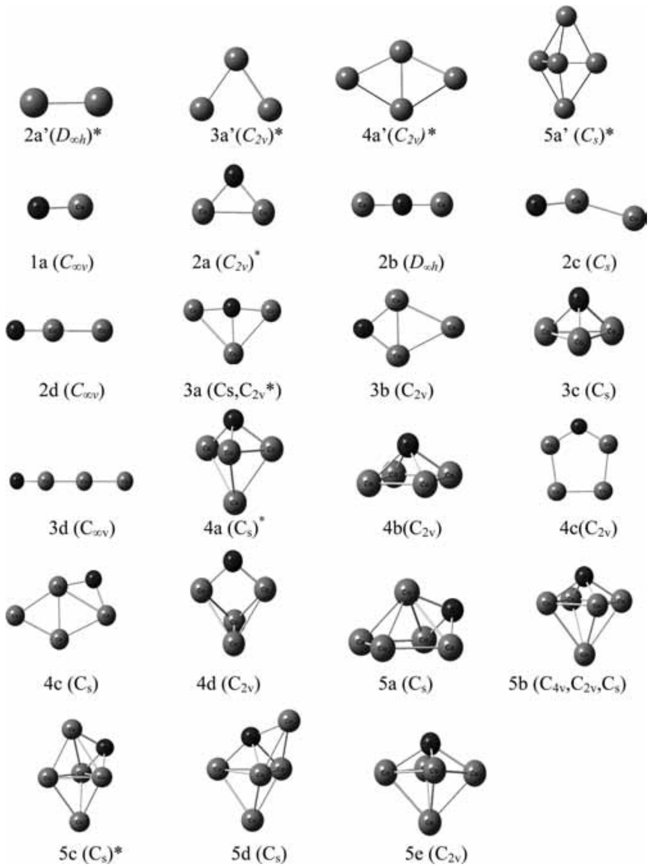

Figure 1. Equilibrium geometries of Co_n and Co_nO ($n = 1-5$) clusters. Asterisks indicate the lowest-energy structures. Gray balls and black balls denote the Co and O atoms, respectively.

TABLE 1: The Calculated Bond Length, Frequency, and Electron Affinity for the Co_2 and CoO Clusters

cluster	method	electronic state	bond length (Å)	electron affinity (eV)	ionization potential (eV)	frequency (cm^{-1})
Co_2	B3LYP	$^7\Sigma_u$	2.111	1.32	6.32	349.8
	EXP		2.31[a]	1.11 ± 0.008[b]	≤ 6.42[b]	290.0[c]
CoO	B3LYP	$^4\Delta$	1.595	1.36	8.17	942.9
	EXP	$^4\Delta$	1.631[d]	1.45(1)[e]	8.57[b]	851.7[f]

[a] Reference 39. [b] Reference 11 and 40. [c] References 41 and 42. [d] Reference 43. [e] Reference 44. [f] Reference 43 and 45.

TABLE 2: Geometries and Total Energies of Co_nO ($n = 1-5$) Clusters[a]

cluster	isomer	sym	spin	state	freq (cm^{-1})	E_T (hartree)	ΔE (eV)
CoO	1a	$C_{\infty v}$	**3/2**	**$^{4}\Delta$**	**942.9**	**−220.1970188**	**0.00**
			1/2		934.2	−220.1392829	1.57
			5/2		741.4	−220.1745700	0.61
Co_2O	2a	C_{2v}	**3**	**$^{7}B_2$**	**146.8**	**−365.3096446**	**0.00**
			0	$^{1}A_1$	208.3	−365.1573633	4.14
			1	$^{3}B_2$	221.5	−365.2832549	0.72
			2	$^{5}B_1$	134.0	−365.3040987	0.15
			4	$^{9}B_2$	143.2	−365.2178922	2.50
	2b	$D_{\infty h}$	0		116.9	−365.1480187	4.40
			1		62.0	−365.2582200	1.40
			2		146.6	−365.2903885	0.52
			3		82.2	−365.2661382	1.18
	2c	C_s	0	$^{1}A'$	52.2	−365.1450134	4.48
			1	$^{3}A''$	59.8	−365.2820663	0.75
			2	$^{5}A'$	77.8	−365.2359084	2.01
	2d	$C_{\infty v}$	0	$^{1}\Sigma$	48.2	−365.1287111	4.92
			1		180.7	−365.2240225	2.33
			2		1.4	−365.2381266	1.95
			3		44.2	−365.256677	1.44
			4		15.7	−365.1805491	3.51
Co_3O	3a	C_{2v}	**7/2**	**$^{8}A_2$**	**47.6**	**−510.4034800**	**0.00**
		C_s	1/2	$^{2}A''$	63.3	−510.3998679	0.10
			3/2	$^{4}A''$	25.1	−510.3638049	1.08
			5/2	$^{6}A'$	131.4	−510.3913378	0.33
			9/2	$^{10}A'$	56.2	−510.3811427	0.61
	3b	C_{2v}	1/2	$^{2}B_2$	119.6	−510.3775684	0.71
			3/2	$^{4}B_2$	55.1	−510.3515015	1.41
			5/2	$^{6}B_1$	140.2	−510.3515719	1.41
	3c	C_s	1/2	$^{2}A''$	208.9	−510.3173311	2.34
			3/2	$^{4}A''$	98.9	−510.3511188	1.42
			5/2	$^{6}A''$	95.7	−510.3942241	0.25
			7/2	$^{8}A''$	83.9	−510.3560845	1.29
	3d	$C_{\infty v}$	1/2		31.7	−510.2980929	2.87
			5/2		44.4	−510.2717622	3.58
Co_4O	4a	C_s	**4**	**$^{9}A'$**	**87.9**	**-655.495258**	**0.00**
			0	^{1}A	86.0	−655.2969159	5.40
			1	$^{3}A''$	90.7	−655.3663025	3.51
			2	$^{5}A'$	52.1	−655.4379718	1.56
			3	$^{7}A''$	75.4	−655.4650527	0.82
			5	$^{11}A''$	48.8	−655.4722313	0.63
	4b	C_{2v}	0	$^{1}A_g$	33.1	−655.1776922	8.64
			1	$^{3}A_2$	14.8	−655.3346738	4.37
			2	$^{5}B_2$	43.2	−655.3420356	4.17
			3	$^{7}A_2$	9.2	−655.4254863	1.90
			4	$^{9}B_1$	79.2	−655.4002740	2.59
			5	$^{11}A_2$	65.0	−655.3403216	4.22
	4c	C_{2v}	0	$^{1}A_1$	50.8	−655.2245411	7.37
			1	$^{3}B_1$	19.9	−655.3325459	4.43
	4c	C_s	2	$^{5}A'$	50.2	−655.4314900	1.74
			3	$^{7}A'$	46.9	−655.4618434	0.91
			4	$^{9}A'$	38.3	−655.4870636	0.22
			5	$^{11}A''$	37.7	−655.4871836	0.22
			6	$^{13}A''$	55.8	−655.4650148	0.82
	4d	C_{2v}	0	$^{1}A_1$	173.3	−655.3079211	5.10
			1	$^{3}B_2$	91.7	−655.3507592	3.93
			2	$^{5}A_2$	92.4	−655.4135539	2.22
			3	$^{7}A_2$	30.0	−655.4023602	2.53
Co_5O	5c	C_s	**11/2**	**$^{12}A''$**	**21.1**	**−800.590625**	**0.00**
			1/2	$^{2}A'$	72.6	−800.4955869	2.59
			3/2	$^{4}A'$	83.2	−800.4901912	2.73
			5/2	$^{6}A'$	74.5	−800.5292045	1.67
			7/2	$^{8}A'$	69.4	−800.5460681	1.21
			9/2	$^{10}A''$	77.3	−800.5512626	1.07
			13/2	$^{14}A'$	66.4	−800.5760002	0.40
	5a	C_s	5/2	$^{6}A''$	20.7	−800.5585318	0.87
			1/2	$^{2}A''$	81.8	−800.5430353	1.29
			3/2	$^{4}A''$	47.5	−800.5347670	1.52
			7/2	$^{8}A'$	66.9	−800.5460649	1.21
	5b	C_{4v}	1/2	$^{2}A_1$	53.5	−800.3941671	5.35
			3/2	$^{4}A_2$	95.5	−800.4431199	4.01
	5b	C_{2v}	5/2	$^{6}A_1$	53.1	−800.5316377	1.61
			7/2	$^{8}A_2$	105.1	−800.4935138	2.64
	5d	C_s	1/2	$^{2}A''$	28.2	−800.4971054	2.54
			3/2	$^{4}A'$	54.8	−800.5211743	1.89
			5/2	$^{6}A''$	70.2	−800.5490673	1.13
			7/2	$^{8}A''$	53.0	−800.522628	1.85
	5e	C_{2v}	1/2	$^{2}A_1$	36.2	−800.5403772	1.37
			3/2	$^{4}B_1$	82.5	−800.4728003	3.21
			5/2	$^{6}B_1$	67.0	−800.4541095	3.71

[a] Sym means point-group symmetry, freq represents the lowest vibrational frequency, E_T denotes the total energies of different Co_nO isomers, and ΔE denotes the relative energy of every isomer compared to that of the lowest-energy isomer for identical-sized cluster.

electronic state of $^7B_2$; the most stable Co_2O geometry is described as O atom replacing one Co atom of the most stable Co_3 cluster.[47] The metastable $D_{\infty h}$ 2b cluster is a linear geometry with O atom being connected directly with two Co atoms (Figure 1). It should be mentioned that the low-lying doublet $D_{\infty h}$ 2b isomer is 0.52 eV higher in total energy than the ground-state 2a isomer. The C_s 2c isomer, which is described as the deformed 2a isomer, is an opened triangular structure, with total energy being higher by 0.75 eV than that of the ground-state 2a isomer. Furthermore, the doublet C_s 2c isomer is lower by 0.691 eV in total energy than the low-lying $C_{\infty v}$ 2d isomer, consequently, the C_s 2c isomer is seen as an intermediate between the C_s 2c and $C_{\infty v}$ 2d forms.

According to the calculated total energies, one finds that the 2c and 2d isomers with O atom being bonded with one cobalt atom are slightly higher in total energies than the 2a and 2b structures. Consequently, the C_{2v} Co_2O cluster with Co−O−Co bridged bond is more stable as compared to the cluster in which the O atom merely is bonded with one Co atom. The calculated adiabatic IP for the septet C_{2v} Co_2O is 8.21 eV. In analogous to that of CoO^+ cluster, the calculated natural populations show that the charge in C_{2v} Co_2O^+ isomer is removed from the two cobalt atoms. This finding is in good agreement with the available experimental results.[11]

Co_3O. Four possible Co_3O isomers with different spin states are optimized and shown in Figure 1. According to the calculated total energy (Table 1), the octet C_{2v} Co_3O 3a isomer is seen as the most stable geometry; Furthermore, the O atom in the 3a isomer is bonded directly with three Co atoms with nonequivalent bond lengths. For the planar C_{2v} 3b cluster, the geometry can be described as one Co atom being capped on the C_{2v} Co_2O 2a cluster above. In other words, the C_{2v} 3b geometry is interpreted as a deformed Co_4 isomer through replacement of one Co atom by O atom.[36,47] Geometrical optimization on the C_{3v} Co_3O cluster turns out that it is not a stable structure. After a relaxation of the high-symmetry C_{3v} geometry along the imaginary frequency to a low-symmetry structure, the stable triangular pyramidal C_s Co_3O 3c isomer is finally yielded.

Specifically, the O atom in the C_s Co_3O 3c geometry is capped on the planar octet C_{2v} Co_3 cluster, and interacts with three Co atoms simultaneously. The linear $C_{\infty v}$ 3d isomer is the highest one in total energy as compared with the 3a, 3b, and 3c isomers. The sextet C_s 3c isomer is lower by 0.46 eV in total energy than the doublet C_{2v} 3b isomer while the sextet C_s 3c is slightly higher by 0.25 eV in total energy than the octet C_{2v} 3a isomer, therefore, the octet C_{2v} 3a isomer is selected as the ground state with electronic state of $^8A_2$. It should be mentioned that the C_s 3c geometry with electronic state being labeled as $^6A''$ character is the metastable isomer.

Co_4O. A variety of possible initial geometries are optimized for the Co_4O clusters. Four stable C_s 4a, C_{2v} 4b, C_s 4c, and C_{2v} 4d geometries are finally obtained, which are selected as the possible ground-state candidates (Figure 1). It needs to be pointed out that the total energy for the four Co_4O isomers decreases as spin S goes from $S = 0$ to $S = 2$ steadily, and the high-spin states for the 4a, 4b, and 4c isomers are calculated. As far as the C_s 4a isomer is concerned, the Co_4O 4a cluster being the most likely candidate for the ground state is yielded after the Co atom is capped on the C_s Co_3O cluster. Apparently, the O atom bonds with three cobalt atoms simultaneously. Geometry optimization on C_s Co_4O 4a isomer exhibits that the nonet state is lower in total energy than other isomers. As spin goes from $S = 0$ to $S = 2$, the C_{2v} 4b isomer is optimized to be the stable geometry, which can be described as the O atom being capped on the most stable planar rectangle nonet C_{2v} Co_4 (4a′) isomer (Figure 1). As can be seen from the findings related to the geometry correlation with the spin of the species considered, the singlet and triplet 4c geometries can be depicted as a planar pentagonal C_{2v} 4c isomer with O substituted for one Co atom of D_{5h} Co_5 cluster;. From the quintet state to the spin state with spin $S = 5$, the C_{4v} 4c geometry begins to be distorted into the low-symmetry C_s 4c geometry, along with the total energy of the C_s 4c cluster decreasing steadily. It should be pointed out that the low-lying septet C_{2v} 4b cluster is apparently higher in total energy than the C_s 4c cluster with spin $S = 5$. As far as the C_{2v} Co_4O 4d is concerned, this geometry is described as one Co atom in the trigonal bipyramidal Co_5 cluster[8] being substituted by one O atom. The calculated results for the C_{2v} 4d isomer show that the total energies decrease gradually with the spin going from $S = 0$ to $S = 2$, and begin to increase at $S = 3$. Apparently, the stable quintet C_{2v} 4d isomer is higher by 2.22 eV in total energy than the nonet C_s 4a cluster.

According to the aforementioned discussion, the nonet C_s 4a isomer is selected as the most stable isomer and ground state, and its electronic state is assigned as $^9A'$.

Co_5O. The C_s 5a geometry is obtained after the O atom is capped on the tetragonal pyramidal C_s Co_5 cluster.[47] The O atom in C_s 5a interacts directly with three cobalt atoms with nonequivalent bond lengths; this phenomenon is similar to that of the most stable Co_4O 4a cluster mentioned above. The doublet and quartet C_{4v} 5b geometries are seen as one Co atom being capped on C_{2v} Co_4O cluster; however, the sextet C_{4v} 5b isomer turns out that it is not a stable structure. After the C_{4v} 5b geometry undergoes a distortion into a low-symmetry geometry, the stable sextet C_{2v} 5b cluster is obtained. With respect to the C_s 5c and C_s 5d isomers, the geometries can be described as O-capped trigonal bipyramidal Co_5 cluster with spin $S = 11/2$ being the most stable isomer[47] and Co-capped trigonal bipyramidal C_s Co_4O 4a cluster, respectively. The total energies for 5a and 5e isomers are decreased as spin goes from $S = 1/2$ to $S = 5/2$, and the higher spin state calculations are needed. Interestingly, the final equilibrium geometry of 5a isomer with $S = 9/2$, $S = 11/2$, and $S = 13/2$ is completely analogous to that of 5c isomer with the same spin states. According to the calculated total energies listed in Table 2, the 5c with spin $S = 11/2$ is more stable than the other isomers, indicating that the 5c isomer with spin $S = 11/2$ is more stable than the others. Consequently, the 5c isomer with electronic state of $\mathbf{^{12}A''}$ is selected as the ground state for Co_5O clusters.

According to the above-mentioned discussions, one concludes that, for Co_nO clusters ($n = 3$, 4, and 5), the stable isomers with O atom being bonded with two Co atoms or four Co atoms simultaneously are less stable than those with O atom being bonded with three Co atoms; the most stable geometries are characteristic as the O atom being bonded with three Co atoms simultaneously. Furthermore, the O atom in the most stable Co_nO ($n = 3-5$) clusters interacting with three Co atoms is the dominant geometry for the small-sized Co_nO clusters. Consequently, the oxygen atom prefers surface-capped cobalt clusters. Based upon the optimized Co_n ($n = 1-5$) geometries (Figure 1), one finds that the incoming oxygen in Co_nO ($n = 1-5$) clusters deforms significantly the geometries of bare Co_n ($n = 1-5$) clusters.

3.2. The Relative Stabilities.

In order to investigate the relative stabilities of the most stable Co_nO ($n = 1-5$) clusters, it is significant to calculate the averaged atomic binding energies ($E_b(n)$) for Co_nO clusters, the fragmentation energies ($D(n,n-1)$)

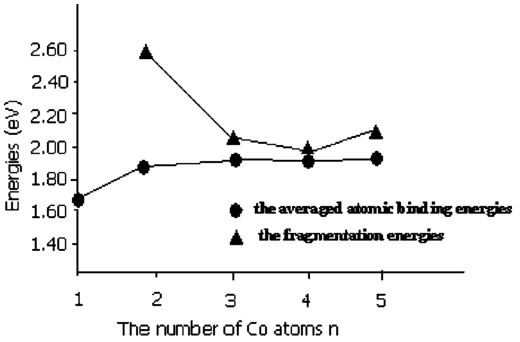

Figure 2. Size dependence of the fragmentation energies and the averaged atomic binding energies of the most stable Co_nO clusters.

TABLE 3: The Calculated Fragmentation Energies ($D(n,n-1)$) and the Averaged Atomic Binding Energies (E_b) of the Most Stable Co_nO ($n = 1-5$) Clusters (Unit: eV)

	$n = 1$	$n = 2$	$n = 3$	$n = 4$	$n = 5$
$D(n,n-1)$	2.596	2.084	2.028	2.126	
$E_b(n)$	1.638	1.957	1.989	1.997	2.018

with respect to removal of one Co atom from the most stable Co_nO clusters. The averaged atomic binding energies and fragmentation energies of Co_nO ($n = 1-5$) clusters are defined as

$$D(n,n-1) = E_T(Co_{n-1}O) + E_T(Co) - E_T(Co_nO)$$

$$E_b(n) = \frac{[E_T(O) + nE_T(Co) - E_T(Co_nO)]}{n+1}$$

where $E_T(Co_{n-1}O)$, $E_T(Co)$, $E_T(O)$, and $E_T(Co_nO)$ denote the total energies for the most stable $Co_{n-1}O$, Co, O, and Co_nO clusters, respectively. The calculated $E_b(n)$ and $D(n,n-1)$ values of the most stable Co_nO ($n = 1-5$) isomers are plotted as the curves of $E_b(n)$ and $D(n,n-1)$ against the corresponding number of the Co atoms in Figure 2 and also summarized in Table 3. It should be mentioned that the features of the size-evolution are intuitively viewed and the peaks of the curve in Figure 2 correspond to those clusters have enhanced local stabilities.

The averaged atomic binding energies of Co_nO clusters are calculated, which are listed in Table 3 and shown in Figure 2. Based on the calculated results, one finds that the averaged atomic binding energy of the most stable Co_nO clusters is increased from $n = 1$ to $n = 5$, Thus, the clusters can continue to gain energy during the growth processes. The calculated fragmentation energies of Co_nO clusters can give the information of relative stabilities of clusters and provide the most stable units. According to the calculated fragmentation energies shown in Figure 2 and listed in Table 3, it is exhibited that the relative stability decreases as the size of cluster n increases from 2 to 4. Furthermore, the relative stability of Co_2O cluster in terms of the calculated fragmentation energy is the biggest among all the small-sized Co_nO clusters, showing that the corresponding cluster has slightly stronger relative stability and has larger abundance in mass spectroscopy in experiment as compared to the corresponding neighbors. Consequently, the particularly most stable geometry can be assigned to be the Co_2O cluster.

3.3. Magnetic Properties. The calculated magnetic moments of the most stable structures are shown in Table 4 and Figure 3. It should be mentioned that the magnetic moment changes discontinuously with the size of clusters. The behavior of the averaged atomic magnetic moments of the lowest-energy small-sized Co_nO clusters is clearly displayed that the averaged atomic magnetic moments for Co_nO clusters are oscillatory decreased with increasing cluster size; this finding is analogous to those of the reported Zr_n clusters.[18] Furthermore, the septet C_{2v} Co_2O structure has the biggest averaged atomic magnetic moment of 2.0 μ_B/atom, while its 2b, 2c, and 2d isomers, however, have values of respectively 1.33, 0.67, and 2.0 μ_B/atom, which means that the magnetic moments or averaged atomic magnetic moments of small-sized Co_nO clusters in terms of the discussions above depend on their geometries and spin states. Moreover, the magnetic effects of the different electrons in the incomplete 3d subshell do not cancel each other as they do in a complete subshell, giving rise to strong magnetism. In addition, it should be mentioned that the calculated magnetic moments for Co,Co_2, Co_3, Co_4, and Co_5 clusters are 3, 6, 7, 8, and 11 μ_B, respectively, which are completely the same as those of Co_nO clusters. Therefore, the oxygen doped Co_n clusters still retain the magnetic properties of bare Co_n clusters.

TABLE 4: HOMO, LUMO, HOMO−LUMO gaps, the Total Magnetic Moment μ_T, and the Average Magnetic Moment μ_A of the Most Stable Co_nO ($n = 1-5$) Clusters

cluster	state	S	HOMO	LUMO	HOMO−LUMO (eV)	μ_T (μ_B)
CoO	$^4\Sigma$	3/2	−0.24760	−0.11118	3.712	3
Co_2O	$^7B_2$	3	−0.22708	−0.12646	2.738	6
Co_3O	$^8A_2$	7/2	−0.17499	−0.09555	2.162	7
Co_4O	$^9A'$	4	−0.17299	−0.07935	2.548	8
Co_5O	$^{12}A''$	11/2	−0.17209	−0.08757	2.300	11

3.4. HOMO and LUMO Properties. The HOMO and LUMO energies as well as the corresponding HOMO−LUMO gaps of Co_nO clusters are tabulated in Table 4 and reflected in Figure 4. Based upon the calculated results, it can be seen that among the most stable Co_nO ($n = 1-5$) clusters the Co_2O and

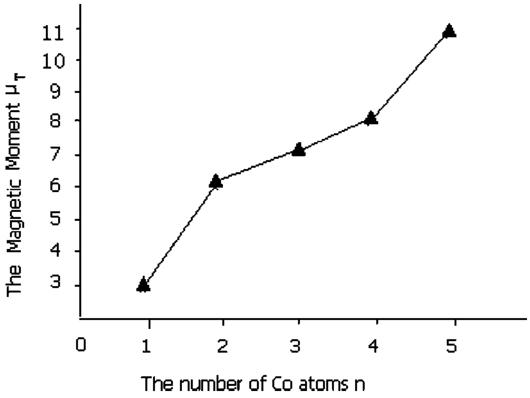

Figure 3. Size dependence of the magnetic moment of the most stable Co_nO clusters.

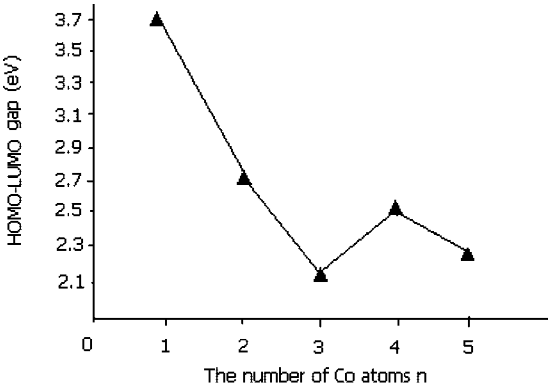

Figure 4. Size dependence of HOMO−LUMO gap of the most stable Co_nO clusters.

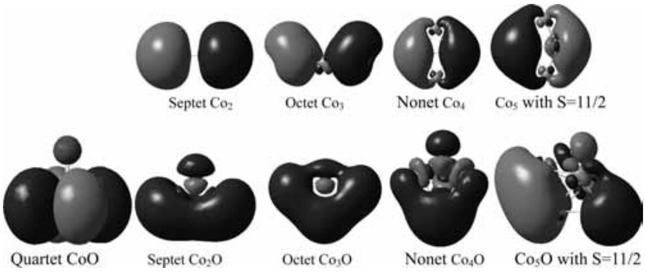

Figure 5. The HOMO states for the most stable Co_nO and Co_n clusters, where the top atom in Co_nO clusters represents the O oxygen.

CoO clusters have bigger HOMO−LUMO gaps than the others. In other words, the chemical stabilities of the septet Co_2O 2a and CoO clusters are stronger in comparison with their neighbors. The HOMO states for the most stable Co_nO clusters are shown in Figure 5. According to the contour maps of the HOMO state of the Co_nO cluster, one finds that the distribution of electron density of the HOMO states for the most stale Co_nO clusters mainly localizes around Co atoms, while the distribution density around O atom is very low, indicating that the hybridization between Co and O atoms is weaker than those between the Co and Co atoms, and their shapes of the HOMO and bonding properties between bare Co_n clusters and Co_nO clusters are obviously different. Furthermore, the Co−Co bondings in the bare Co_n clusters are the localized σ-type bonds or partly delocalized σ-type bonds while the bondings among Co−Co atoms in the Co_nO clusters are completely the delocalized σ-type bonds. Consequently, the hybridization between Co and O atoms should be responsible for the variation of electronic properties of Co_n clusters causing by the adsorbed O atom.

In order to reveal the variation of electronic properties of Co_nO clusters resulting from the incoming oxygen atom, the adiabatic electron affinities (AEA) of the most stable Co_n and Co_nO ($n = 3$ and 4) clusters are calculated. The calculated AEAs for Co_4 and Co_4O clusters are respectively 1.34 and 0.93 eV, and 0.9 and 1.42 eV for the respective Co_3 and Co_3O clusters. The calculated results indicate that the calculated AEA for Co_4 is in good agreement with experimental result (1.4 eV)[29] while the calculated AEA for Co_4O deviates slightly from the experimental measurement, and that the calculated AEAs for Co_3 and Co_3O clusters are reasonable based on the experimental measurements of EAs in ref 29. In other words, the incoming oxygen atom causes little influence on the electronic properties of bare small-sized cobalt clusters; this finding is in good agreement with the previous experimental prediction on the Co_nO^- clusters.[29]

4. Conclusions

The systematic investigations of the Co_nO ($n = 1-5$) clusters with various spin states are performed at the UB3LYP level by using GEN basis sets. The total energies, equilibrium geometries, and stabilities of Co_nO ($n = 1-5$) clusters, together with fragmentation energies and averaged atomic binding energies, are presented and discussed. All calculated results can be summarized as follows: (1) The most stable Co_nO clusters show that the O atom prefers the surface-capped Co_n pattern and interacts with three Co atoms for the most stable Co_nO ($n > 2$) clusters. In other words, the O atom prefers the oxygen surface-capped pattern. (2) The relative stabilities of Co_nO ($n = 1-5$) clusters in terms of calculated fragmentation energies are discussed, showing that the Co_2O cluster is the most stable structure. (3) The calculated averaged atomic magnetic moments of the small-sized Co_nO clusters indicate that the averaged atomic magnetic moment is oscillatorily decreased with the cluster size being increased, however, the C_{2v} Co_2O structure has the biggest averaged atomic magnetic moment of 2.0 μ_B/atom. Furthermore, the most stable Co_n ($n = 1-5$) clusters keep the same spin as those of Co_nO clusters, indicating that the oxygen doped Co_n clusters still retain the magnetic properties of bare Co_n clusters and the incoming oxygen atom causes minor influence on the magnetic properties of Co_n clusters. (4) The calculated HOMO−LUMO gaps indicate that the most stable Co_2O and CoO clusters have stronger chemical stabilities as compared to their neighbor sizes of clusters, and that the distribution of electron density of the HOMO states for the most stable Co_nO clusters mainly localizes around Co atoms while the distribution around O atom is very low. Their shapes of the HOMO and bonding properties between bare Co_n clusters and Co_nO clusters are obviously different. The experimental and our calculated results on electron affinities indicate that the incoming O atom in Co_nO clusters provides a small influence on the electronic properties of bare Co_n clusters. This finding is in good agreement with experimental measurement of threshold binding energy features on the charged Co_nO^- clusters.[29]

Acknowledgment. This work is supported by Chinese National Scientific Fund (9850290013), the HP computational center of National Synchrotron Radiation Laboratory of USTC and SCC of USTC of China.

References and Notes

(1) Molek, K. S.; Reed, Z. D.; Ricks, A. M.; Duncan, M. A. *J. Phys. Chem. A* **2007**, *111*, 8080.
(2) Feyel, S.; Scharfenberg, L.; Daniel, C.; Hartl, H.; Schröder, D.; Schwarz, H. *J. Phys. Chem. A* **2007**, *111*, 3278.
(3) Asmis, K. R.; Sauer, J. *Mass Spectrom. Rev.* **2007**, *26*, 542.
(4) Tono, K.; Terasaki, A.; Ohta, T. *J. Chem. Phys.* **2006**, *124*, 184311.
(5) Molek, K. S.; Jaeger, T. D.; Duncan, M. A. *J. Chem. Phys.* **2005**, *123*, 14.
(6) Cui, X.; Harrion, H.; Han, J. G. *J. Chem. Phys.* **2002**, *117*, 1077.
(7) Veliah, S.; Xiang, K. H.; Pandey, R.; Recio, J. M.; Newsam, J. M. *J. Phys. Chem. B* **1998**, *102*, 1126.
(8) Han, J. G.; Ren, Z. Y.; Lu, B. Z. *J. Phys. Chem. A* **2004**, *108*, 5100.
(9) Wang, L. S.; Wu, H.; Desai, S. R. *Phys. Rev. B* **1996**, *53*, 8028.
(10) Andrews, L.; Chertihin, G. V.; Ricca, A.; Bauschlicher, C. W., Jr. *J. Am. Chem. Soc.* **1996**, *118*, 467.
(11) Liu, F. Y.; Li, F. X.; Armentrout, P. B. *J. Chem. Phys.* **2005**, *123*, 064304.
(12) Citra, A.; Chertihin, G. V.; Andrews, L.; Neurock, M. *J. Phys. Chem. A* **1997**, *101*, 3109.
(13) Andersson, M.; Persson, J. L.; Rosén, A. *J. Phys. Chem.* **1996**, *100*, 12222.
(14) Danset, D.; Manceron, L. *J. Phys. Chem. A* **2003**, *107*, 11324.
(15) Tjernbergyx, O.; Chiaiayk, G.; Karlssony, U. O.; Grootz, F. M. F. *Condens. Matter.* **1997**, *9*, 9863.
(16) Castell, M. R.; Dudarev, S. L.; Briggs, G. A. D.; Sutton, A. P. *Phys. Rev. B* **1999**, *59*, 11.
(17) Langell, M. A.; Anderson, M. D.; Carson, G. A.; Peng, L.; Smith, S. *Phys. Rev. B* **1999**, *59*, 7.
(18) Wang, C. C.; Zhao, R. N.; Han, J. G. *J. Chem. Phys.* **2006**, *124*, 194301.
(19) Clouthier, D. J.; Huang, G.; Merer, A. J.; Friedman-Hill, E. J. *J. Chem. Phys.* **1993**, *99*, 6336.
(20) Nakao, Y.; Hirao, K.; Taketsugu, T. *J. Chem. Phys.* **2001**, *114*, 18.
(21) Freas, R. B.; Dunlap, B. I.; Waite, B. A.; Compana, J. E. *J. Chem. Phys.* **1987**, *86*, 3.
(22) Uzunova, E. L.; Nikolov, G. S.; Mikosch, H. *J. Phys. Chem. A* **2002**, *106*, 4104.
(23) Morse, M. D. *Chem. Rev.* **1986**, *86*, 1049.
(24) Chertihin, G. V.; Citra, A.; Andrews, L.; Bauschlicher, C. W. *J. Phys. Chem. A* **1997**, *101*, 8793.
(25) Guo, B. C.; Kerns, K. P.; Castleman, A. W. *J. Phys. Chem.* **1992**, *96*, 6931.
(26) Jacobsont, D. B.; Freiser, B. S. *J. Am. Chem. Soc.* **1986**, *108*, 27.

(27) Danset, D.; Alikhani, M. E.; Manceron, L. *J. Phys. Chem. A* **2005**, *109*, 97.

(28) Kapiloff, E.; Ervin, K. M. *J. Phys. Chem. A.* **1997**, *101*, 8460.

(29) Pramann, A.; Koyasu, K.; Nakajima, A.; Kaya, K. *J. Phys. Chem. A* **2002**, *106*, 4891.

(30) Danset, D.; Alikhani, M. E.; Manceron, L. *J. Phys. Chem. A* **2005**, *109*, 105.

(31) Gutsev, G. L.; Rao, B. K.; Jena, P. *J. Phys. Chem. A* **2000**, *104*, 5374.

(32) Becke, A. D. *Phys. Rev. A* **1983**, *38*, 3098.

(33) Lee, C.; Yang, W.; Parr, R. G. *Phys. Rev. B* **1988**, *27*, 785.

(34) Wadt, W. R.; Hay, P. J. *J. Chem. Phys.* **1985**, *82*, 284.

(35) Han, J. G.; Zhao, R. N.; Duan, Y. H. *J. Phys. Chem. A* **2007**, *111*, 2148.

(36) Castro, M.; Jamorski, C.; Salahub, D. R. *Chem. Phys. Lett.* **1997**, *271*, 133.

(37) Yoshida, H.; Terasaki, A.; Kobayashi, K.; Tsukada, M.; Kondow, T. *J. Chem. Phys.* **1995**, *102*, 15.

(38) Rodrıguez-López, J. L.; Aguilera-Granja, V.; Michaelian, K.; Vegad, A. *J. Alloys Compd.* **2004**, *93*, 369.

(39) Frish, M. J.; Trucks, G. W.; Schlegel, H. B.; *GAUSSIAN 03*; Gaussian, Inc.: Pittsburgh, PA, 2003.

(40) Kant, A.; Strauss, B. *J. Chem. Phys.* **1964**, *41*, 3806.

(41) Leopold, D. G.; Lineberger, W. C. *J. Chem. Phys.* **1986**, *85*, 51.

(42) Dilella, D. P.; Limm, W.; Lipson, R. H.; Moskovits, M.; Taylor, K. V. *J. Chem. Phys.* **1982**, *77*, 5263.

(43) Chuang, Y. Y.; Schmid, R.; Chang, Y. A. *Met. Trans. A* **1985**, *16*, 153.

(44) Adam, A. G.; Azuma, Y.; Barry, J. A.; Huang, G. J.; Michael, P. J.; Lyne, M. A. J.; Schröder, J. O. *J. Chem. Phys.* **1987**, *86*, 5231.

(45) Li, X.; Wang, L. S. *J. Chem. Phys.* **1999**, *111*, 8389.

(46) Merer, A. J. *Annu. Rev. Phys. Chem.* **1989**, *40*, 407.

(47) Fan, H. J.; Liu, C. W.; Liao, M. *Chem. Phys. Lett.* **1997**, *273*, 353.

JP8080244